Review of the Influence of 'A' Site Doped-Substitution on the Structural, Magnetic and Electrical Properties of La-Based Manganites

Nur 'Ain Hamdan[1] and Zakiah Mohamed[2*]
[1]Center of Foundation Studies, Universiti Teknologi Mara, UiTM Dengkil, 43800, Selangor, Malaysia
[2*]Faculty of Applied Sciences, Universiti Teknologi Mara, UiTM Shah Alam, 40450, Selangor, Malaysia
[*]Corresponding author (e-mail: zakiah626@uitm.edu.my, ainhamdan@uitm.edu.my)

The discovery of colossal magnetoresistance (CMR) effect on manganite has led to increased attention to explore the main properties of these materials. A review study was conducted to understand the influence of 'A' site doping on lanthanum (La)-based manganites and evaluate their structural, magnetic and electrical properties. In general, lanthanum, a rare earth element, can be used to create $La_{1-x}A_xMnO_3$, where A represents monovalent ions (Na, K or Ag) or divalent ions (Ba, Pb, Sr or Ca) that are octahedrally coordinated by oxygen ions. This work also discusses the structure, phase diagram, double-exchange mechanism and phase separation of CMR manganites. La-based parent compounds doped at the A site (Na, K, Ba, Sr) were synthesised by a conventional solid-state method. When *x* increases, the CMR increases due to the competition between charge ordering and double exchange. At high temperatures or high applied magnetic fields, manganites exhibit extraordinarily large CMR in response to the transition of insulator–metal and paramagnetic–ferromagnetic regions at the same temperature. The substitutions of A doping could increase the lattice distortion between the ions and cause size mismatch. The electrical resistivity results reveal that manganites act as an insulator behaviour at above the metal–insulator transition temperature T_{MI} and as metal at below T_{MI}. The resistivity increases when the A site concentration in the compound increases.

Keywords: Manganites; doping; structural; magnetic; electrical

Perovskite manganites belong to the family of compound $R_{1-x}A_xMnO_3$, where R is a trivalent rare earth ion (R = La^{3+}, Pr^{3+}, Nd^{3+}, Eu^{3+} and Bi^{3+}) and A is a monovalent ion (K^+, Na^+, Ag^+, Li^+) or a divalent ion (Pb^{2+}, Cu^{2+}, Sr^{2+}, Ca^{2+}). These materials have gained increased research attention due to their special physical properties, such as colossal magnetoresistance (CMR), phase separation (ps), charge orbital (co), and orbital ordering (oo) as well as magnetic and electrical properties [1-2]. With their promising properties, they have potential for future magnetic and technology applications, such as sensors, spin valve, magnetic refrigeration and storage devices [3-4]. A large change in the application of external magnetic field is referred to the CMR property. The CMR effect has two main types, namely, extrinsic and intrinsic. Firstly, the extrinsic CMR effect requires a low magnetic field or low field magnetoresistance (LFMR) and describes the interfaces and grain boundaries in a compound. Secondly, the intrinsic CMR effect requires a very high magnetic field up to 1T, which is non-viable for device applications [5]; this effect explains the double-exchange (DE) mechanism of manganese ions between Mn^{3+} and Mn^{4+}. LFMR has good interconnection between grains on magnetic and transport properties [6], mixed between noncollinear spin structure and large number of grain boundaries [6-7] and obtain a high saturation moment with the smallest grain size [7-8]. Undoped $LaMnO_3$ is an antiferromagnetic insulator because of the superexchange coupling between Mn^{3+} ions. When doped with specific concentrations of divalent ions at the A site, $LaMnO_3$ displays electrical transition from metallic to insulator behaviour at the metal–insulator transition temperature T_{MI} accompanied by magnetic transition from ferromagnetic to paramagnetic phase at the Curie temperature T_C [9-10]. Manganese ions exist in the parent compound as Mn^{3+} or Mn^{4+}. In general, the valence states of $R^{3+}Mn^{3+}O_3^{2-}$ and $A^{2+}Mn^{4+}O_3^{2-}$ are formulated from mixed-valence oxides $(R_{1-x}^{3+}A_x^{2+})(Mn_{1-x}^{3+}Mn_x^{4+})O_3$ in solid solution. Mixed-valence Mn^{3+} and Mn^{4+} ions are present during A-site doping into La-based manganites. The equal ratio of Mn^{3+}/Mn^{4+} (1:1) leads to charge ordering (CO) and competes with DE interaction, and CO localises electron charges and retards electrons from hoping from one side to another. As such, manganite exhibits insulator or metallic behaviour. Mixed-valence Mn ions mainly influence CMR; other factors that affect CMR are ionic size mismatch, Mn-O bond length and Mn-O-Mn bond angle. Doping A-site metal ions into

165   Nur 'Ain Hamdan and Zakiah Mohamed

Review of the Influence of 'A' Site Doped-Substitution on the Structural, Magnetic and Electrical Properties of La-Based Manganites

La-based perovskite manganite can change the crystal structure, ion size and ion valence state. The double exchange (DE) effect of Mn^{3+}-O^{2-}-Mn^{4+} is an important topic to study the magnetic and transport properties of perovskite manganites [11-12]. The e_g electrons are delocalised and reconcile the ferromagnetic interaction between localised t_{2g} spins due to their strong hybridisation with the oxygen 2p states. Therefore, a variety of magnetic structures can be substituted at the A site in La manganite because of the competition between antiferromagnetic superexchange and ferromagnetic double-exchange interactions [13]. DE interactions occur between the exchange of Mn^{3+} and Mn^{4+} ions, favouring the ferromagnetic metallic (FMM) state; meanwhile, Jahn–Teller (JT) interactions involving Mn^{3+} ions favour the paramagnetic insulating (PMI) behaviour [14-15]. Furthermore, the interconnections between the configuration of local spins and the dynamic of e_g carrier responses contribute to electronic properties involving temperature and magnetic-dependent transition from metal to non-metal behaviour. Scholars conducted monovalent ion substitutions with A-site doped ions, such as Ag^+, Na^+, K^+, Li^+, etc. into La manganite to induce the metal–insulator transition at low substitution levels. Only few works focused on $La_{1-x}Ag_xMnO_3$ [16-20], where Ag substitution increased the T_{MI} to higher temperatures and decreased the resistivity near T_{MI} due to strong DE interactions between Mn^{3+} and Mn^{4+} ions [16-20]. Ag doping creates an electron scattering mechanism, in which electrons are transported within grains boundaries, leading to increased electron conductivity among grains [16,20]. The metallic Ag ion can modify Mn spin disorder and produce extrinsic MR at low temperatures [16, 20], thereby influencing the electric transport and MR properties of manganites. Further research should focus on the substitution of ions for A-site doping into La-based manganite by using divalent ion and trivalent ion to produce $La_{0.7}Ba_{0.18}Sr_{0.12}MnO_3$ [15], $La_{1-x}Ca_xMnO_3$ [17], $La_{0.67-x}Bi_xSr_{0.33}MnO_3$ [21], $La_{0.67-x}Eu_xCa_{0.35}MnO_3$ [22], $La_{0.7-x}Nd_xBa_{0.3}MnO_3$ [23] and $La_{0.7-x}Pr_xPb_{0.3}MnO_3$ [24]. Moreover, the tolerance factor τ may influence the CMR properties of the A-site ion-doped manganites. It can be calculated by $\tau = (<r_A> + <r_O>/\sqrt{2}(<r_B> + <r_O>))$ where $<r_A>, <r_B>$ and r_O represent the average ionic radius of A, B and O sites, respectively. The magnitude of τ indicates the degree of lattice between the A-O layer and its neighbouring B-O layers and reflects the degree of distortions of MnO_6 octahedra [25-27]. Increasing the distortions of the MnO_6 octahedra will increase the mismatch between A-O and B-O layers but decrease the tolerance factor. In CO divalent-doped manganites, the charge-ordering transition temperature and the mismatch between A-O and B-O layers increase, strengthening the CO state [25-26]. Substitution with Sr, which has a larger ionic radius, with divalent CO, such as in $La_{0.5}Ca_{0.5-x}Sr_xMnO_3$ [27] manganite, increases the τ, weakens the CO state and induces the FMM state. This work reviews the influence of A-site doping on the structural, magnetic and electrical properties of lanthanum (La)-based perovskite manganites.

EXPERIMENTAL

Conventional solid-state reaction is commonly used to synthesise polycrystalline manganite materials by pre-sintering the compound powder at 750 °C to 950 °C for 10–25 hours after grinding. Before finishing the samples, the powder was pressed into pellets and re-sintered in a furnace at 900 °C–1300 °C for 15–30 hours. The furnace was then cooled down to the room temperature. XRD technique was used to analyse the phase of the samples with Cu-K_α radiation ($\lambda = 1.5418$ Å) at 2θ. Structural parameters were determined by Rietveld method using GSAS and EXPGUI software [28]. Magnetic and electrical properties were examined under different values of magnetic field. Polycrystalline manganite was synthesised using the previously reported floating-zone (FZ) method in $La_{1-x}Sr_xMnO_3$ [29]. The raw materials of polycrystalline sample were weighed in an appropriate ratio, mixed and stirred with acetone for 1 hour in a ball mill. The mixture was heated in air by using a FZ furnace at 1200 °C for 24 hours. A feed rod was built to a sample with 5 mm diameter, cylindrical shape and 80 mm length under pressure of 2 ton/cm^2 before heating the mixture in air at 1200 °C for 24 hours. The rod was rotated at 50 rpm in opposite direction, and the melted zone was scanned in a vertical direction at 9 mm/hr speed. The crystal structure was examined by XRD method with Cu K_α radiation. The polycrystalline samples of $La_{0.65}Ca_{0.35-x}Li_xMnO_3$ manganite were synthesised using Pechini method [30]. Before weighing the samples, traces of water and absorbed gasses were expelled by heating $CaCO_3$ and Li_2CO_3 in a hot air oven at 373 K and La_2O_3 at 1273 K for 5 hours in the furnace. The sample materials were dissolved with 3 N HNO_3, stirred at 353 K to obtain metal nitrates and added with citric acid. Polyethylene glycol was poured with citric acid as polymerising agent before it was heated on a hot plate at 353 K to form a gel. The obtained gel was dried in a hot air oven at 523 K to produce dry powder before it was calcined at 773 K. The powder was ground, pressed into pellets and calcined at 1373 K for 24 hours. The phase and structure of the samples were examined by XRD with Cu-K_α radiation ($\lambda = 1.5418$ Å) at 2θ. Structural parameters were analysed by Rietveld method using GSAS software.

RESULTS AND DISCUSSION

1.   Structural Properties

In general, the CMR parent compound $LaMnO_3$ is an ideal cubic perovskite. The structure of $LaMnO_3$ has a three-dimensional network of vertex with face-centred cubic lattice and A-sites occupied by La cations on the corners as cubic structure and B-sites occupied by Mn ions in the centre of the unit cell surrounded with six

166   Nur 'Ain Hamdan and Zakiah Mohamed

Review of the Influence of 'A' Site Doped-
Substitution on the Structural, Magnetic and
Electrical Properties of La-Based Manganites

oxygen ions called as MnO_6 octahedra. The cubic structure in La-based manganites can be modified into other symmetrical structures, such as rhombohedral in $La_{1-x}Ag_xMnO_3$ [31], orthorhombic in $La_{1-x}Ca_xMnO_3$ [32] or trigonal in $La_{0.7}Ba_{0.18}Sr_{0.12}MnO_3$ [15], through cooperative titling of MnO_6 octahedra and displacement of cations or distortion of MnO_6 octahedra. Increasing the doping concentration of A-site ions (Na, K, Bi, Ba, Sr) into La parent compound may change the size mismatch and lattice distortions between the ions, thereby affecting the lattice parameters, lattice volume, Mn-O bond distance and Mn-O-Mn angles after analysis using Rietveld refinement. This distortion leads to the Jahn–Teller effect during the deformation of the MnO_6 octahedra existing permanently to the high spin $(S = 2)$ Mn^{3+} with double degeneracy of the e_g orbital [11-12]. For example, the XRD pattern of $La_{0.65}Ca_{0.35-x}Li_xMnO_3$ $(0 \leq x \leq 0.15)$ [33] shows all the samples are in a single phase without any impurity at the peak with an orthorhombic Pbnm space group. The atomic position in the orthorhombic Pbnm reveals that La, Ca and Li are fixed at the 4c site (x, y, 0.25), Mn was fixed at the 4b site (0, 0.5, 0), O_1 was fixed at the 4c site (x, y, 0.5) and O_2 was fixed at the 8d site (x, y, z). When the concentration x of Li doping is increased, the lattice parameters (a, b, c) increase, ultimately increasing the unit lattice volume from 228.29 $Å^3$ $(x = 0)$ to 231.67 $Å^3$ $(x = 0.15)$. The increase in the unit lattice volume is due to the cationic disorder because of the increased Li concentration reported earlier [34]. When the Li^+ ion is substituted to the Ca^{2+} ion, oxidation occurs between Mn^{3+} and Mn^{4+}, leading to the existence of Mn^{3+}/Mn^{4+} pairs. These pairs influence the DE interaction, which plays a role in the ferromagnetic properties of the manganites. The reduction of the DE interaction Mn^{3+}-O-Mn^{4+} exists during Li

doping at $x > 0.05$, thereby increasing the Mn^{4+} content above 40% and favouring the Mn^{4+}-O-Mn^{4+} SE interaction. Any movement on the valence state of the Mn ions is attributed to PM to FM and insulating to metallic state [9-11]. In another study on $La_{1-x}Li_xMnO_3$ $(x = 0.10, 0.15, 0.20, 0.30)$ manganite [35], the XRD structure changed from rhombohedral to ($R\overline{3}C$, Z = 2; $x \leq 0.15$) to orthorhombic (Pbnm, Z = 4; $x \geq 0.20$). This change increased the lattice distortion and bending of the Mn-O-Mn bond. In this perovskite structure, lattice distortion is due to the deformation of the MnO_6 octahedra from the JT effect, which is inherent to high-spin $(S = 2)$ Mn^{3+} ions. When the system is crystallised in the Pbnm space group with orthorhombic symmetry at the optimum concentration $(x = 0.3)$, the transition from PM to FM state occurs at 250 K, thereby changing the insulating state to metallic state [36]. The substitution of Sr^{2+} for Ca^{2+} induces the structural transformation from the orthorhombic to the rhombohedral structure and increases the value of T_C [37]. The partial replacement of Ca^{2+} by N^+ or K^+ can lead to the structural transformation from the orthorhombic to the rhombohedral symmetry and increase the value of T_C with alkali content [38]. In 1950, Zener proposed the mechanism of double exchange (DE) and explained that the electron splitting e_g on Mn^{3+} can hop to a neighbouring ion site Mn^{4+} [39]. This mechanism is shown in Figure 1. Based on the DE mechanism, three electrons of the Mn^{3+} are in the t_{2g} level, and one electron lays in the e_g level. The spin alignment among the four electrons is ruled by Hund's coupling. Otherwise, the e_g level is vacant in the Mn^{4+} ion. An oxygen 2p orbital acts as a bridge between the two Mn^{3+} and Mn^{4+} to form DE interaction. Thus, Mn^{3+} e_g electron hops to the Mn^{4+} ion via the O^{2-} ion.
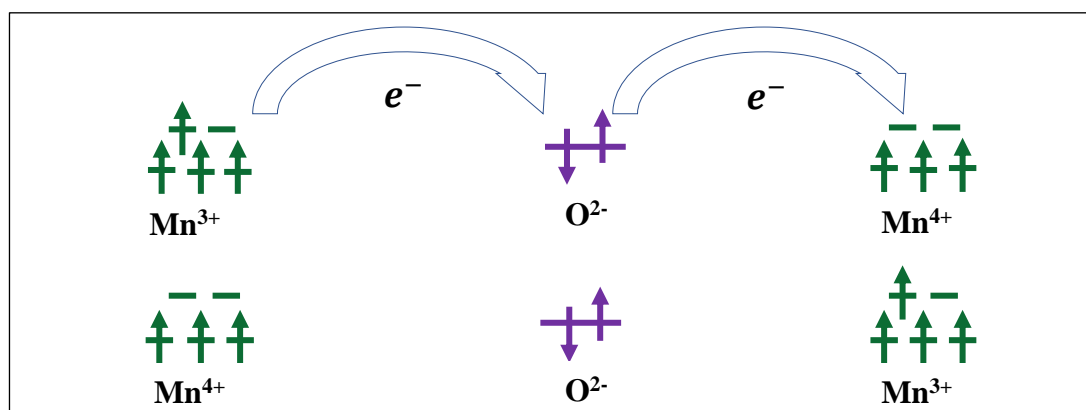

Figure 1. Schematic diagram of double-exchange (DE) mechanism.

167 Nur 'Ain Hamdan and Zakiah Mohamed

Review of the Influence of 'A' Site Doped-
Substitution on the Structural, Magnetic and
Electrical Properties of La-Based Manganites

2. Magnetic Properties

As one of the magnetic properties that belong to perovskites, transition temperature can be modified by doping the A-site ions from different groups, such as monovalent, divalent or trivalent ions. As a function of temperature and doping, various magnetic transitions are associated with changes in electrical conductivity. Table 1 shows that the Curie temperature (T_C) from La parent compounds increases the magnetic field due to DE mechanism, producing a giant magnetoresistance. The mixed-valence manganites in $LaMnO_3$ exhibits transition from paramagnetic (PM) to ferromagnetic (FM) state at T_C ranging from 100 K to 360 K depending on the type of materials. According to theory, changes in the magnetic properties of manganites are due to the magnetic coupling between Mn^{3+}/Mn^{4+} pairs, thereby changing the DE interaction. Additionally, the reduction of the mobility among the electrons results in JT coupling, reduces the DE interaction. Furthermore, increasing T_C is attributed to the strength of DE ferromagnetic interactions. The bonding angle Mn-O-Mn increases due to structure phase transformation, and its T_C value depends on the bandwidth of the conduction e_g electron. When the concentration of A-site doped ion is increased, the volume ratio between Mn^{4+}/Mn^{3+} increases, thereby increasing the ferromagnetic DE and the value of T_C. Some studies reported that the increase in size mismatch among A-site cations decreases the T_C and T_{MI}. As the size mismatch increases, the degree of oxygen displacement increases, thereby promoting the localisation between charge carrier, disturbing the distortion of MnO_6 octahedral and decreasing the T_C and T_{MI}. A factor of τ may attribute to changes in T_C and T_{MI} and modify the MnO_6 octahedral distortions when A-site doped ion is substituted. The substitution of large ion at the A site affects the CO suppression and FMM state. Increasing τ may reduce the distortion of MnO_6 octahedra, influencing the alignment spins of Mn^{3+}/Mn^{4+}, improving the e_g transfer via $Mn^{3+}-O-$

Mn^{4+} interaction and enhancing the DE mechanism. Studies revealed that the transformation from the insulating behaviour to the metallic behaviour is induced by the applied field [32-35]. In 1950s, the first series of divalent substituted $La_{1-x}Ca_xMnO_3$ compound with FM metallic state was obtained [40]. The phase diagram of the same compound $La_{1-x}Ca_xMnO_3$ has been reviewed [41-42]. The range of T_C between 160 K to 272 K for $0 < x < 5$ doped materials exhibit PM to FM transition. The plot of the in-phase susceptibility $\chi^{'}$ versus temperature (T) for $0 < x < 0.20$ samples can lead to further understanding of the magnetic properties (Figure 2) [43]. According to this paper, $La_{0.70-x}Bi_xAgMnO_3$ exhibits FM to PM phase transition at $x < 0.2$. At $x = 0.2$, two minimum peaks appear due to magnetic inhomogeneity induced by Bi^{3+} ion substitution [44]. Increasing the concentration of Bi^{2+}-doped ions ($x = 0, 0.10, 0.15, 0.20$) will decrease the T_C due to the weakening of the ferromagnetic behaviour as a result of Bi substitution [45-46]. $La_{1-x}K_xMnO_3$ compound ($0 < x < 0.20$) also possesses PM to FM transition at 230 K$< T_C <$ 334 K [47]. However, in another work, FM phase transition in $La_{1-x}Sr_xMnO_3$ was not observed at $x \le 0.05$ [29]. Increasing the concentration of Sr^{2+} ions doped from $x \le 0.10$ to $x \le 0.40$ increases the T_C between 145 K to 371 K. The internal DE and molecular magnetic moment of the material strongly affect the Curie temperature (T_C) and the maximum magnetic entropy change (ΔS_M^{max}). Another study on $La_{1-x}K_xMnO_3$ reported that increasing the K^+ doping concentration for $0.00 < x < 0.20$ increases the T_C range between 206 to 309 K [48]. All the same $La_{1-x}K_xMnO_3$ have increased $|\Delta S_M^{max}| = 2.72$ J/kg K for $x = 0.05$ to 3.00 J/kg K for $x = 0.15$ close to their T_C, respectively. Furthermore, in $La_{1-x}Cd_xMnO_3$ compounds, where ($x = 0.3, 0.4$ and 0.5), increasing the doping concentration of Cd^{2+} ions in La manganites enhances the T_C from 253 K to 270 K and increases the maximum magnetic entropy change to 2.33 J/kgK at the applied field of 10 kOe [49]. Hence, $La_{1-x}Cd_xMnO_3$ exhibits PM to FM phase transition.

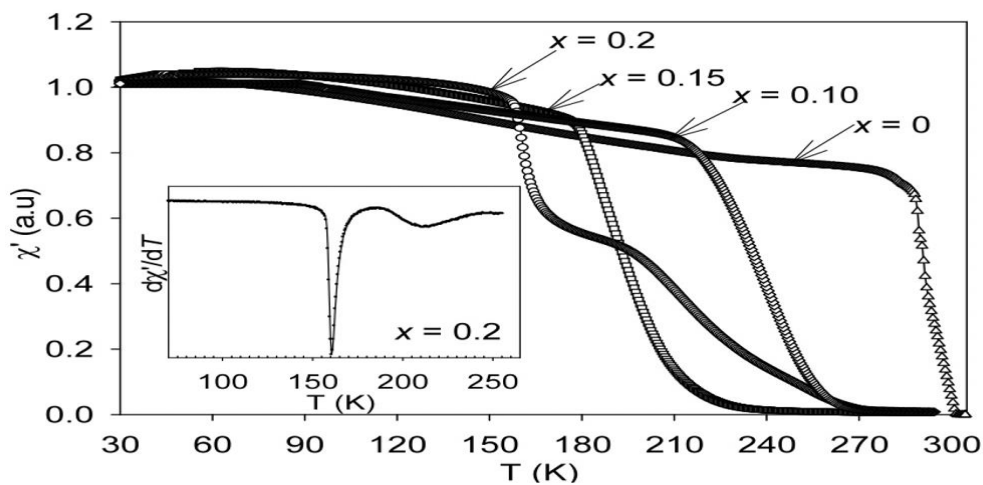**Figure 2.** Ac susceptibility component, $\chi^{'}$ as a function of temperature for $La_{0.70-x}Bi_xAgMnO_3$ in ($x = 0, 0.10, 0.15$ and 0.20) samples [43].

168 Nur 'Ain Hamdan and Zakiah Mohamed

Review of the Influence of 'A' Site Doped-
Substitution on the Structural, Magnetic and
Electrical Properties of La-Based Manganites

Table 1. Comparison of reported Curie temperature and magnetic entropy changes values among La-based manganites with A-site substitutions.

Composition	T_C (K)	ΔS_m (J / kgK)	Reference
$La_{0.9}Na_{0.1}MnO_3$	218	1.53	[50]
$La_{0.925}Na_{0.075}MnO_3$	195	1.32	[50]
$La_{0.835}Na_{0.165}MnO_3$	342	1.22	[50]
$La_{0.80}Na_{0.20}MnO_3$	334	1.96	[50]
$La_{0.95}Ag_{0.05}MnO_3$	214	1.10	[31]
$La_{0.95}Ag_{0.05}MnO_3$	214	1.10	[51]
$La_{0.80}Ag_{0.20}MnO_3$	278	3.40	[31]
$La_{0.80}Ag_{0.20}MnO_3$	300	2.40	[51]
$La_{0.78}Ag_{0.22}MnO_3$	306	2.90	[52]
$La_{0.75}Ag_{0.25}MnO_3$	306	1.52	[31]
$La_{0.75}Ag_{0.25}MnO_3$	306	1.52	[51]
$La_{0.70}Ag_{0.30}MnO_3$	306	1.35	[31]
$La_{0.70}Ag_{0.30}MnO_3$	306	1.35	[51]
$La_{0.80}Ca_{0.20}MnO_3$	230	5.50	[53]
$La_{0.75}Ca_{0.25}MnO_3$	224	4.70	[53]
$La_{0.75}Ca_{0.25}MnO_3$	224	4.70	[54]
$La_{0.70}Ca_{0.30}MnO_3$	256	1.38	[53]
$La_{0.68}Ca_{0.32}MnO_3$	272	2.90	[53]
$La_{0.60}Ca_{0.40}MnO_3$	263	5.00	[55]
$La_{0.55}Ca_{0.45}MnO_3$	238	1.90	[53]
$La_{0.90}Pb_{0.10}MnO_3$	160	0.53	[56]
$La_{0.80}Pb_{0.20}MnO_3$	294	1.22	[56]
$La_{0.70}Pb_{0.30}MnO_3$	352	0.96	[56]
$La_{0.87}Sr_{0.13}MnO_3$	197	5.80	[52]
$La_{0.845}Sr_{0.155}MnO_3$	234	6.60	[52]
$La_{0.880}Sr_{0.120}MnO_3$	152	6.00	[57]
$La_{0.865}Sr_{0.135}MnO_3$	200	4.40	[57]
$La_{0.845}Sr_{0.155}MnO_3$	235	6.70	[57]
$La_{0.815}Sr_{0.185}MnO_3$	280	7.10	[57]
$La_{0.80}Sr_{0.20}MnO_3$	305	7.90	[57]
$La_{0.67}Sr_{0.33}MnO_3$	348	1.69	[58]
$La_{0.65}Sr_{0.35}MnO_3$	305	2.12	[59]
$La_{2/3}Sr_{1/3}MnO_3$	370	1.50	[60]

3.   Electrical Properties

In general, the CMR parent compound $LaMnO_3$ is classified as an electrical insulator at all temperatures. It can exhibit antiferromagnetic (AFM) transition with different Neel temperatures (T_N). A previous study on neutron diffraction experiment reported that $LaMnO_3$ and $CaMnO_3$ obtained T_N at 140 K and 131 K, respectively [13]. The chemical compound $R_{1-x}A_xMnO_3$ exhibits metal to insulator transition at $0.10 < x < 0.50$. The peak temperature from the curve graph of electrical resistivity versus temperature indicates the M-I temperature (T_{MI}) transition of the compound. The graph shows three regions to identify the types of temperature transition: high temperature for insulator region, low temperature for metal region and critical

169   Nur 'Ain Hamdan and Zakiah Mohamed

Review of the Influence of 'A' Site Doped-Substitution on the Structural, Magnetic and Electrical Properties of La-Based Manganites

temperature for intermediate region. For instance, $La_{0.7}Bi_xAg_{1-x}MnO_3$ exhibits metal to insulator transition at T_{MI} of 253 K for $x = 0$ sample under an applied magnetic field of 0 T (Figure 3) [43]. However, under the same applied magnetic field at 0 T, the T_{MI} decreases rapidly between 254.8 K to 136.3 K when Bi^{2+} doped into 0.15 and 0.20 samples, respectively. Increasing the doping concentration of the Bi^{2+} ion ($x = 0, 0.15$ and 0.20) into $La_{0.70-x}Bi_xAgMnO_3$ increases the electrical resistivity but decreases the T_{MI} and T_C due to increased localisation of e_g electrons and weakened DE mechanism [45-46]. In $La_{1-x}Li_xMnO_3$, two samples for $x = 0.10$ and $x = 0.15$ exhibit metal–insulator (M-I) transition and its T_C increases from 210 K to 240 K when the Li^+ ion doping concentration is increased [35]. A negative MR ratio $\sim$26% was obtained near T_c with applied field of 0.8 T. Increasing the K^+ doping amount enhances magnetic entropy changes, whereas increasing the T_C in $La_{1-x}K_xMnO_3$ decreases the Mn-O distance. The substitution of smaller ion La^{3+} ion (ionic radii $\sim$1.016 Å) with the larger K^+ ion (ionic radii $\sim$1.33 Å) in $La_{1-x}K_xMnO_3$ increases the average ionic radius of the La site, thereby producing crystallographic distortions and enlarging the Mn-O-Mn bond angle. In further studies on doping divalent ions at the A site in $La_{1-x}Sr_xMnO_3$, the local crystal lattice becomes distorted from the ideal cubic structure to the orthorhombic and rhombohedral structures, leading to changes in the Mn-O bond distance and the Mn^{3+}-O^{2-}-Mn^{4+} bond angle because the La^{3+} ion is substituted with the larger Sr^{2+} ion [61]. Meanwhile, $La_{1-x}Sr_xMnO_3$ possesses metal–insulator (M-I) transition due to some localisation effects [29]. A previous study on $La_{1-x}Cd_xMnO_3$ confirmed that the substitution of a larger La^{3+} ion (ionic radii $\sim$1.216 Å) with a smaller Cd^{2+} ion (ionic radii $\sim$1.016 Å) increases the Mn^{4+} and favours the DE interactions [49].

CONCLUSSION

This paper reviews the influence of A-site doping into La-based perovskite manganites on their structural, magnetic and electric properties. When the A-site doping ion is substituted by monovalent or divalent ions, such as Na^+, K^+, Ca^{2+}, Sr^{2+} or Pb^{2+}, increasing the sample concentration between 0.00 to 0.20 may affect the lattice parameters of the compound due to differences in size radius between the La ion and A-site doped ion. Furthermore, increasing the concentrations of the A-doped substituted samples into La leads to ferro-magnetic–metal behaviour in the lower temperature region ($T < T_{MI}$) and paramagnetic–insulator behaviour in the higher temperature region ($T > T_{MI}$).
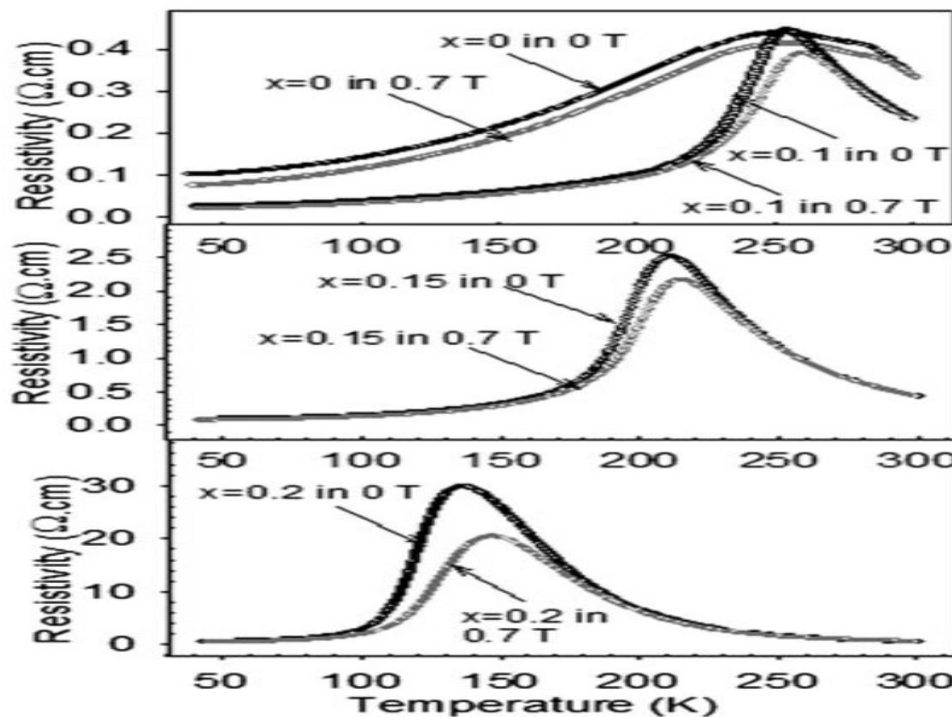

Figure 3. Electrical resistivity (ρ) as a function of temperature for $La_{0.70-x}Bi_xAgMnO_3$ ($x = 0$, 0.15 and 0.2) under applied magnetic field of in 0 T and 0.7 T [43].

170   Nur 'Ain Hamdan and Zakiah Mohamed

Review of the Influence of 'A' Site Doped-
Substitution on the Structural, Magnetic and
Electrical Properties of La-Based Manganites

REFERENCES

1. Ramirez, A. P. (1997) Colossal Magnetoresistance. *Journal of Physics Condense Matter*, **9**, 8171–8199.

2. Navin, K. & Kurchania, R. (2017) Structural, magnetic and transport properties of the $La_{0.7}Sr_{0.3}MnO_3$-ZnO nanocomposites. *Journal of magnetism & magnetic materials*, **448**, 228–235.

3. Yue-Wei Yin, Muralikrishna Raju, Wei-Jin Hu, Xiao-Jun Weng, Ke Zou, Jun Zhu, Ziao-Guang Li, Zhi-Dong Zhang & Qi Li (2012) Multiferroic tunnel junctions. *Frontiers of physics*, **7**, 380–385.

4. Maftoon-Azad, L., Yazdanpanah, Z. & Mohamadi-Baghmolayi (2015) A perturbed hard sphere chain equation of state for refrigerants. *Journal of Molecular Liquids*, **208**, 388–393.

5. Sadhu, A. & Bhattachharyya, S. (2014) Enhanced low-field magnetoresistance in $La_{0.71}Sr_{0.29}MnO_3$ nanoparticles synthesized by the nonaqueous so-gel route. *Journal chemistry of materials*, **26**, 1702–1710.

6. Andress, A. De, García-Hernández, M., Martinez, J. L. & Prieto, C. (1999) Low- temperature magnetoresistance in polycrystalline manganites: connectivity versus grain size. *Journal of applied physics letters*, **74(25)**, 3884–3886.

7. Martinez, B., Obradors, X., Balcells, Li., Rouanet, A. & Monty, C. (1998) Low Temperature Surface Spin-Glass Transition in γ-Fe2O3 Nanoparticles. *Journal of physical review letters*, **80(1)**, 181–184.

8. Dey, P. & Nath, T. K. (2005) Enhance grain surface effect on temperature-dependent behavior of spin-polarized tunnelling magnetoresistance of nanometric manganites. *Journal of applied physics letters*, **87(16)**, 3884–3886.

9. Coey, J. M. D., Viret, M. & Von Molnar, S. (1999) Mixed-valence manganites. *Advanced in Physics*, **48(2)**, 167–293.

10. Jonker, G. H. (1956) Magnetic compounds with perovskite structure IV conducting and non-conducting compounds. *Physica XXII*, **22**, 707–722.

11. Kubo, K. & Ohata, N. (1972) A quantum theory of double exchange. *Journal of Physical Society of Japan*, **33(1)**, 21–32.

12. Gennes, D. P. -G. (1960) Effects of double exchange in magnetic crystals. *Physical Reviews*, **118(1)**, 141–154.

13. Wollan, E. O. & Koehler, W. E. (1955) Neutron diffraction study of the magnetic properties of the series of perovskite- type compound [(1-x)La,xCa]MnO_3. *Physical Reviews*, **100(2)**, 545–563.

14. Anderson, P. W. & Hasegawa, H. (1955) Consideration on double exchange. *Physical Review*, **100(2)**, 675–681.

15. Hwang, H., Cheong, S. -W., Radaelli, P. G., Marizeo, M. & Batlogg, B. (1995) Lattice effects on magnetoresistance in doped $LaMnO_3$. *Physical Review Letters*, **75(5)**, 914–917.

16. Ye, S. L., Song, W. H., Dai, J. M., Wang, K. Y., Wang, S. G., Chang, Z. L., Du, J. J., Sun, Y. P. & Fang, J. (2002) Effect of Ag substitution on the transport property and magnetoresistance of $LaMnO_3$. *Journal of Magnetism and Magnetic Materials*, **248(1)**, 26–33.

17. Monoranjan Kar & Ravi, S. (2004) Electrical resistivity and ac susceptibility studies in $La_{1-x}Ag_xMnO_3$. *Materials Science and Engineering B.*, **110(1)**, 46–51.

18. Ravi, S. & Monoranjan Kar (2004) Study of magneto-resistivity in $La_{1-x}Ag_xMnO_3$ compounds. *Physica B*, **348(1-4)**, 169–176.

19. Battabyal, M. & Dey, T. K. (2004) Thermal conductivity of silver doped lanthanum manganites between 10 K and 300 K. *Journal of Physics and Chemistry of Solids*, **65(11)**, 1895–1900.

20. Kalyana Lakshimi, P. & Venugopal Reddy, P. (2009) Electrical behavior of some silver-doped lanthanum-based CMR materials. *Journal of Magnetism and Magnetic Materials*, **321(9)**, 1240–1245.

21. Cheng, Z. X., Silver, T. M., Li, A. H., Wang, X. L. & Kimura, H. (2004) Effect of progressive substitution of La^{3+} by Bi^{3+} on the structure, magnetic and transport properties of $La_{0.67}Sr_{0.33}MnO_3$. *Journal of Magnetism and Magnetic Materials*, **283(2-3)**, 143–149.

22. Li, Z., Zhao, Q., Fan, W. & Zhan, J. (2011) Porous SnO_2 nanospheres as sensitive gas sensors for volatile organic compounds detection. *Nanoscale*, **3(4)**, 1646–1652.

171 Nur 'Ain Hamdan and Zakiah Mohamed

Review of the Influence of 'A' Site Doped-Substitution on the Structural, Magnetic and Electrical Properties of La-Based Manganites

23. Wang, Z., Ni, G. & Che, Y. (2012) Magneto-caloric effect in perovskite manganite $La_{0.65}Nd_{0.05}Ba_{0.3}MnO_3$ with double metal-insulator peaks. *J Supercond Nov Magn.*, **25(2)**, 533–539.

24. Chen, H. Z., Young, S. L., Chen, Y. C., Lance Horng & Shi, J. B. (2003) Magnetic and transport properties of $La_{0.7-x}Pr_xPb_{0.3}MnO_3$. *Physica B.*, **329-333**, 729–730.

25. Joel, C., Jean-Francois, B. & Ulrike, L. (2005) Development of new materials for spintronics. *Comptes Rendus Physique*, **6(9)**, 977–996.

26. Smolyaninova, V. N., Lofland, S. E., Hill, C., Budhani, R. C., Serpil Gonen, Z., Eichhorn, B. W. & Greene, R. L. (2002) Effect of A-site cation disorder on charge ordering and ferromagnetism of $La_{0.5}Ca_{0.5-y}Ba_yMnO_3$. *Journal of Magnetism and Magnetic Materials*, **248(2)**, 348–354.

27. Sundaresan, A., Paulose, P. L., Mallik, R. & Sampathkumaran, E. V. (1998) Bandwidth-controlled magnetic and electronic transitions in $La_{0.5}Ca_{0.5-x}Sr_xMnO_3$ ($0 \leq x \leq 0.5$) distorted perovskite. *Physical Review B.*, **57(5)**, 2690–2693.

28. Toby, B. H. (2001) EXPGUI, a graphical user interface for GSAS. *Journal of Applied Crystallography*, **34(2)**, 210–213.

29. Urushibara, A., Moritomo, Y., Arima, T., Asamitsu, A., Kido, G. & Tokura, Y. (1995) Insulator-metal transition and giant magnetoresistance in $La_{1-x}Sr_xMnO_3$. *Physical Review B.*, **51(20)**, 14103–14109.

30. Lakshmi, Y. K., Venkataiah, G., Vithal, M. & Reddy, P. V. (2008) Magnetic and electrical behavior of $La_{1-x}A_xMnO_3$ (A = Li, Na, K and Rb). *Physica B.*, **403(18)**, 3059–3066.

31. Tang, T., Gu, K. M., Cao, Q. Q., Wang, D. H., Zhang, S. Y. & Du, Y. W. (2000) Magnetocaloric properties of Ag substituted perovskite-type manganese oxides. *Journal of Magnetism & Magnetic Materials*, **222(1-2)**, 110–114.

32. Radaelli, P. G., Cox, D. E., Marezio, M., Cheong, S. -W., Schiffer, P. E. & Ramirez, A. P. (1995) Simultaneous structural, magnetic and electronic transitions in $La_{1-x}Ca_xMnO_3$ with x =0.25 and 0.50. *Physical Review*, **75(24)**, 4488–4491.

33. Verma, M. K., Sharma, N. D., Sharma, S., Choudhary, N. & Singh, D. (2020) Structural and magneto-transport properties of Li-substituted $La_{0.65}Ca_{0.35-x}Li_xMnO_3$ ($0 \leq x \leq 0.15$) CMR manganites. *Journal of Alloys and Compounds*, **814**, 152279–152289.

34. Martinez, R., Lide, M. & Paul, A. J. (1996) Cation disorder in magnetoresistive manganese oxide perovskites. *Physical Review B.*, **54(22)**, 15622–15625.

35. Ye, S. L., Song, W. H., Dai, J. M., Wang, S. G., Wang, K. Y., Yuan, C. L. & Sun, Y. P. (2000) Effect of Li substitution on the crystal structure and magnetoresistance of $LaMnO_3$. *Journal of Applied Physics*, **88(10)**, 5915–5919.

36. Millis, A. J. (1998) Lattice effects in magneto-resistive manganese perovskites. *Nature*, **393 (6672)**, 147–150.

37. Ulyanov, A. N., Gusakov, G. V., Borodin, V. A., Starostyuk, N. Y. & Mukhin, A. B. (2001) Ferromagnetic ordering temperature and internal pressure in manganites $La_{0.7}Ca_{0.3-x}Sr_xMnO_3$. *Journal of Solid State Communication*, **118(2)**, 103–105.

38. Maatar, S. C., Nassri, R. M., Koubaa, W. C., Koubaa, M. & Cheikhrouhou, A. (2015) Structural, magnetic and magnetocaloric properties of $La_{0.8}Ca_{0.2-x}Na_xMnO_3$ ($0 \leq x \leq 0.2$) manganites. *J. Solid State Chem.*, **225**, 83–88.

39. Zener, C. (1951) Interaction between d-shells in the transition metals II ferromagnetic compounds of manganese with perovskites structure. *Physical Review*, **82(3)**, 403–405.

40. Jonker, G. H. & Van Santen, J. H. (1950) Ferro-magnetic compounds of manganese with perovskite structure. *Physica*, **16(3)**, 337–349.

41. Schiffer, P., Ramirez, A. P., Bao, W. & Cheong, S. -W. (1995) Low temperature magnetoresistance and magnetic phase diagram of $La_{1-x}Ca_xMnO_3$. *Physical Review Letters*, **75(18)**, 3336–3339.

42. Sun, J. Z., Gallagher, W, K., Duncombe, P. R., Krusin-Elbaum, L., Altman, R. A., Gupta, A., Yu Lu, Gong, G. Q. & Xiao Gang. (1996) Observation of large low-field magnetoresistance in tri-layer perpendicular transport devices made using doped manganite perovskites. *Applied Physics Letters*, **69(21)**, 3266–3268.

43. Ghani, M. A., Mohamed, Z. & Yahya, A. K. (2012) Effects of Bi substitution on magnet and transport properties of ceramics. *J Supercon Nov Magn.*, **25**, 2395–2402.

44. Walsh, M. C., Foldeaki, M., Giguere, A., Bahadur, D., Manhal, S. K. & Dunlap, R. A. (1998). Magnetic and electronic properties of the magnetoresistive perovskites $La_{0.67}Bi_xCa_{0.33}MnO_3$. *Physica B: Condensed Matter*, **253(1-2)**, 103–110.

45. Cheng, Z. X., Silver, T. M., Li, A. H., Wang, X. L. & Kimura, H. (2004) Effect of progressive substitution of La^{3+} by Bi^{3+} on the structure,

172   Nur 'Ain Hamdan and Zakiah Mohamed

Review of the Influence of 'A' Site Doped-
Substitution on the Structural, Magnetic and
Electrical Properties of La-Based Manganites

magnetic and transport properties of $La_{0.67}Sr_{0.33}MnO_3$. *Journal of Magnetism and Magnetic Materials*, **283(2-3)**, 143–149.

46. Zhao, Y. D., Jonghyuk, P., Jung, R. J., Noh, H. J. & Oh, S. J. (2004) Structure, magnetic and transport properties of $La_{1-x}Bi_xMnO_3$. *Journal of Magnetism and Magnetic Materials*, **280(2-3)**, 404–411.

47. Zhong, W., Chen, W., Ding, W. P., Zhang, N., Hu, A., Du, Y. W. & Yan, Q. J. (1999) Synthesis, structure and magnetic entropy change of poly-crystalline $La_{1-x}K_xMnO_{3+\delta}$. *Journal of Magnetism and Magnetic Materials*, **195(1)**, 112–118.

48. Das, S. & Dey, T. K. (2007) Magnetic entropy changes in polycrystalline $La_{1-x}K_xMnO_3$ perovskites. *Journal of Alloys and Compounds*, **440 (1-2)**, 30–35.

49. Dhahri, J., Dhahri, A., Oumezzine, M, Dhahri, E., Said, M. & Vincent, H. (2009) Magnetocaloric properties of Cd-substituted perovskite-type manganese oxides. *Journal of Alloys and Compounds*, **467(1-2)**, 44–47.

50. Zhong, W., Chen, W., Ding, W., Zhang, N., Du, Y. & Yan, Q. (1998) Magnetocaloric properties of Na-substituted perovskite-type manganese oxides. *Solid State Communication*, **106(1)**, 55–58.

51. Hien, N. T. & Thuy, N. P. (2002) Preparation and magnetocaloric effect of $La_{1-x}Ag_xMnO_3$ ($x = 0.10$-0.30) perovskite compounds. *Physica B: Condense Matter*, **319(1-4)**, 168–173.

52. Szewcyzk, A., Gutowska, M. & Piotrowski, K. (2003) Direct and Specific Heat Study of Magnetocaloric Effect in $La_{0.845}Sr_{0.155}MnO_3$. *Journal of Applied Physics*, **94 (3)**, 1873–1876.

53. Phan, M. H. & Yu, S. C. (2007) Review of the Magnetocaloric Effect in Manganite Materials. *Journal of Magnetism Magnetic Materials*, **308**, 325–340.

54. Guo, Z. B., Zhang, J. R., Huang, H., Ding, W. P. & Du, Y. W. (1997) Large magnetic entropy changes in $La_{0.75}Ca_{0.25}MnO_3$. *Applied Physics Letters*, **70(7)**, 904–905.

55. Bohigas, X., Tejada, J., Marinez-Sarrion, M. L., Tripp, S. & Black, R. (2000) Magnetic and calorimetric measurements on the magnetocaloric effect in $La_{0.60}Ca_{0.40}MnO_3$. *Journal of Magnetism Magnetic Materials*, **208(1-2)**, 85–92.

56. Min, S. G., Kim, K. S., Yu, S. C., Suh, S. H. & Lee, S. W. (2005) Magnetocaloric properties of $La_{1-x}Pb_xMnO_3$ ($x = 0.1, 0.2, 0.3$) compounds. *IEEE Transactions on Magnetics*, **41(10)**, 2760–2762.

57. Szewcyzk, A., Gutowska, M. & Dabrowski, B., Plackowski, T., Danilova, N. P. & Gaidukov, Yu, P. (2005) Specific Heat Anomalies in $La_{1-x}Sr_xMnO_3$ ($0.12 \leq x \leq 0.2$). *Physical Review B.*, **71(22)**, 2244321–2244327.

58. Morelli, D. T., Mance, A. M., Mantese, J. V. & Micheli, A. L. (1996) Magnetocaloric properties of doped lanthanum manganite film. *Journal of Applied Physics*, **79(1)**, 373–375.

59. Phan, M. H., Tian, S. B., Hoang, D. Q., Yu, S. C., Nguyen, C. & Ulyanov, A. N. (2003) Large magnetic entropy changes above 300 K CMR materials. *Journal of Magnetism and Magnetic Materials*, **258-259**, 309–311.

60. Mira, J., Rivas, J., Hueso, L. E., Rivadulla, L. & Lopez Quintela, M. A. (2002) Drop of magneto-caloric effect related to the change from first to second order magnetic phase transition in $La_{2/3}(Ca_{1-x}Sr_x)_{1/3}MnO_3$. *Journal of Applied Physics*, **91(10)**, 8903–8905.

61. McBride, K., Cook, J., Gray, S., Felton, S., Stella, L. & Paulidi, D. (2016) Evaluation of $La_{1-x}Sr_xMnO_3$ $0 < x < 0.40$ synthesized via a sol-gel method as mediators for magnetic fluid hyperthemia. *Royal Society of Chemistry*.